Mechanical Engineering Department
University of Texas at Dallas (UTD)
800 West Campbell Rd., Richardson, TX75080

To Reviewers and Editors, December 21, 2019

Please find the copy of the manuscript entitled "***Kraken: A wirelessly controlled octopus-like hybrid robot utilizing stepper motors and fishing line artificial muscles for grasping underwater***", Y. Almubarak, M. Schmutz, M. Perez, S. Shah, and Y. Tadesse to be considered for publication in your International Journal of Intelligent Robotics and Applications.

In this paper, we present a new octopus-like robot that is capable of operating in a swimming pool and grasping objects using its soft flexible arms, which will contribute to the bioinspired design of vehicles for ocean monitoring as well as other underwater activities. The arms are uniquely designed to actuate in multimodal fashion (curling, twisting, and bending), which can grasp intricate geometries delicately and exhibit excellent actuation characteristics. We used a hybrid actuation system consisting of stepper motors and novel artificial muscles (*Twisted and Coiled Polymer, (TCP)* muscles). The polymer muscles are tailored to have a heating element (TCP_{FL}) and they were embedded in silicone elastomer to actuate the robot arm. Our TCP_{FL} arm shows tremendous potential for the advancement in soft robotics as it occupies less physical space, inexpensive for swarm systems, and high strain. We showed several characteristics of the robot and the flexible arm with embedded muscles that will contribute to the state of the art. We showed a wireless connection and untethered actuation of the robot that is implemented to enhance maneuverability, especially in areas that exterior cables would otherwise become unpractical. We have provided several videos and supplementary files along with the main results. The highlights and the contribution of the paper are listed below.

- A modular, bioinspired, robust, octopus-like robot named Kraken is presented, with 3-D printed watertight dome-like exterior as a housing for all the electronics and hardware of the robot. It has three layers, the actuation unit, buoyancy unit, and electronics unit. This robot can be potentially used for rescue missions in a swimming pool. It can swim along with humans (safe human–robot interaction) or perform other underwater manipulations.
- Six different arm configurations, offering multi-dimensional actuation options for grasping several objects safely are demonstrated. The arms are controlled by the hybrid actuation system consisting of stepper motors and TCP_{FL} actuators, which were not demonstrated before.
- A buoyancy control system is included. It has an air bladder attached to the top surface of the robot. This will allow vertical swimming underwater upon inflation and deflation. A wireless joystick controller is incorporated for complete hands-off control of the robot using a lithium-ion battery. The robot can operate continuously for a total time of 45 minutes in a swimming pool.
- Extensive studies of the TCP_{FL} polymer muscles that were embedded in the silicone elastomer for use in underwater grasping will help other researchers to use the data and create similar robots. We identified the bending mechanics and the heat transfer mechanism of the muscles for correlating the basic physics for underwater application. We also performed fluid-structure simulation studies to understand the motion and flow behavior of the robot during swimming.

We hereby declare that the materials presented in this article are results of original work and are not being submitted for publication elsewhere.
Thank you for your consideration.

With best regards

Yonas Tadesse, PhD,
Associate Professor of Mechanical Engineering,
The University of Texas at Dallas (UTD).
800 West Campbell Rd., Richardson, TX75080-3021
Office: ECSW 3.150E; Office Phone: 972-883-4556
http://me.utdallas.edu/people/tadesse.html ; http://www.utdallas.edu/~yonas.tadesse/

Title

Kraken: A wirelessly controlled octopus-like hybrid robot utilizing stepper motors and fishing line artificial muscles for grasping underwater

Authors

Yara Almubarak[1], Michelle Schmutz[1], Miguel Perez[1], Shrey Shah[1], and Yonas Tadesse[1*]

Affiliations

[1]Humanoid, Biorobotics and Smart Systems (HBS) Laboratory, Mechanical Engineering Department, Jonsson School, The University of Texas at Dallas, Richardson, USA.

*Corresponding Author: Yonas.tadesse@utdallas.edu

Abstract

Underwater exploration requires suitable robotic systems capable of maneuvering, manipulating objects, and operating untethered in complex environmental conditions. Traditional robots have been used to perform many tasks underwater. However, traditional robots have limited degrees of freedom, manipulation capabilities, portability, and disruptive interactions with aquatic life. Research in soft robotics seeks to incorporate ideas of the natural flexibility of aquatic species into man-made technologies to improve the current capabilities of robots using biomimetics. In this paper, we present a novel design, fabrication, and testing results of an underwater robot (Kraken) that manipulates objects by mimicking the arm movement of an octopus. To control the arm motion, Kraken utilizes a hybrid actuation technology consisting of stepper motors and twisted and coiled polymer fishing line muscles. TCPs are becoming one of the promising actuation technologies due to their high actuation stroke, high force, light weight, and is inexpensive. We have studied numerous arm stiffness configurations tailored to operate in different modalities (curling, twisting, bending etc.), to control the shape of the tentacles and grasp irregular objects delicately. Kraken uses an onboard battery, a wireless programmable joystick, a buoyancy system for depth control, all housed in a three-layer 3D printed dome-like structure. Here, we present Kraken fully functioning underwater in an Olympic size swimming pool (field test) for grasping objects using its servo actuated arms and other test results on TCP_{FL} actuated arms in a laboratory setting.

1. Introduction

The field of robotics deals in large with inhospitable environments wherein it is either impossible or very difficult for a person to operate in. One such environment is the high pressure aquatic environment in which human physiology makes it practically impossible for a person to operate in without the assistance of either robots or other machinery. In this environment, even robots have a hard time dealing with both the high water pressure due to the water and the adaptability needed to deal with the myriad of obstacles present in an aquatic environment. The adaptability of a robot is mainly determined by the way it moves and actuates its functional parts, and for a robot intended to function and explore underwater, the adaptability is a significant factor. For the purposes of improving the adaptability of robots beyond that provided by typical motor driven actuation, research is being performed into different bioinspired robotics utilizing novel actuators or artificial muscles. Several actuation technologies have been studied for robotics application such as electromagnetic (EM), pneumatic (PM), hydraulic (HA), piezoelectric (PZT), shape memory alloy (SMA), dielectric elastomer (DE), electroactive polymers (EAPs), and their composite forms. None of them meets the requirement of bioinspired robots design and development. For example, conflicting properties such as low cost and high performance in stress, strain, energy density, life cycle, efficiency, and frequency are difficult to get in one actuation technology. However, tradeoffs have been made in the design and developments of many robots. Twisted and coiled polymer fishing line muscles have been first introduced in 2014 by Haines et al. [1] as a new class of smart materials from The University of Texas at Dallas (UTD). These artificial muscles contract or expand when heated depending on the way they are manufactured. These inexpensive actuators were presented to have a high actuation stroke up to 50%, while lifting heavy loads at 1 MPa, and offering a high energy density of 5.4 kW/kg. Later, new structures were presented by Haines et al.2016, which could even provide 200% reversible strain [2]. The application of twisted and coiled polymer (TCP) actuators such as fishing line (TCP_{FL}) and silver-coated (TCP_{Ag}) has a wide range of contributions especially in the bio-inspired robotics. We have been designing and developing several robots in the last few years using these actuators, TCP_{Ag} [3-5]. The TCP actuators are inexpensive, easily replaceable, are being used in various harsh environments, and are fully functional when exposed in underwater environments. We aimed to design and develop an octopus-like robot utilizing TCPs for the arms due to their benefits in soft robotics. Additionally, we used conventional motors to make a hybrid system for the tendon driven arms. Our approach in design is to try to mimic the

octopus to some extent, but not the entire working mechanism and swimming principles, instead adapting only the flexible arms of the octopus, and to then test the basic motion characteristics in underwater environment.

Tendon based manipulators play a vital role in continuum robotics, which consists of tendons passed through backbone structures. These tendon based systems that are commonly used in continuum robots and biomimetic manipulations are achieved by applying force to tendons using motors, actuators, or other sources [6]. Unique robots have been presented in the literature that mimic certain animals or the flexible structures of animals found in nature. Octoarm is presented as a robotic arm inspired from the octopus [7]. It has 12 degrees of freedom, which utilizes McKibben pneumatic actuators. A biomimetic robotic earthworm was presented that uses shape memory alloys (SMA) for locomotion [8]. In another study, an artificial musculoskeletal system simulating a ball and socket joint is developed using TCP_{FL} actuators [9]. The actuating force of the system in [9] comes from the electrical current running through the TCP_{FL} actuator, as well as the elastic composition of the joint, allowing the system to bend at various angles. The ability of robotic structures to bend and turn similar to biomimetic movements offers a unique opportunity to operate in obstacle filled environments as suggested in [10]. Another example in the field of bio-inspired robots is a robotic hand that can control its fingers independently by opening and closing each finger. The movement of the robot hand as shown in [11,12] is powered by the TCP_{Ag} arranged throughout the hand in a configuration similar to the one found in a human hand. Electricity is then passed through the TCP_{Ag} muscles, or "tendons" in this case, causing them to actuate [11]. In another related study, an artificial elephant nose is presented that has high bending that can be used for rescue missions. The elephant nose-like structure is designed to provide aid such as food and water to victims stuck under debris effect by phenomena such as earthquakes [13].

Progress has also been made in expanding the potential for further applications of TCP actuators, particularly in force amplification. Simeonov et al. [14] has made several TCP muscles by weaving and braiding them together to induce optimal performance. To develop biomimetic robots, the advancement of soft robotic technology, control, and motion is required. Smart actuators such as dielectric elastomers (DE), ionic polymer-metal composite (IPMCs), piezoelectric motors, and shape memory alloys (SMA) provide promising technologies in creating these robots. They behave with repeatable performance, they have been studied for many years (matured), some of them operate at high frequency, and are compact in size; however, they are expensive, and some of them operate at a very high voltage. In comparison, this new TCP technology has numerous advantages such as low cost, light weight, and high actuation strain [1].
Unique biomimetic systems have been presented in recent years. A biohybrid skeletal joint system was presented that can bend up to 90° and perform pick up and drop off tasks [15] also a similar approach was shown for jellyfish like robot [16]. A bioinspired dual stiffness origami gripper is also presented [17]. Many researchers have also presented soft, silicone skin embedded with sensors and actuators such as temperature sensors [18], force sensors [19], pressure sensors [20], and TCP_{Ag} muscles [3]. Soft, platinum-cured silicone is moldable and flexible. Other types of soft skin are also developed, such as "e-skin," that can wirelessly interact with users [21]. The embedding process of sensors and actuators in soft silicone elastomer eliminated the use of extra rigid space that could preclude the movement of the robot, and reduces the risk factor of failure, making it a more reliable option, particularly because of its low maintenance needs. The moldability of silicone allows for the fabrication of more realistic, smoother, biomimetic shapes, therefore the silicone elastomer shows great promise for soft robotics. Calisti et al. [22] showed a simple octopus-like arm to test its functional anatomy. Several mockups were made using different materials and cable arrangement. It was shown that the soft elastomer EcoFlex 00-30 filled with water demonstrates the most satisfying actuation behavior. The biohybrid approach is very interesting; however, it is not practical for field robotics. Therefore, alternatives such as silicone elastomers and actuators are better choice for soft robots.

Several research results have been presented in the field of underwater robotics, robots with swimmers or with grippers. The Kraken is known as a legendary cephalopod-like sea monster. This creature is often portrayed in fiction as a "giant squid" that is very strong and able to swallow ships, whales, and any obstacle it may encounter. This squid like creature is able to stay submerged underwater for days [23]. Our octopus-like robot (**Fig.1**) was deliberately named Kraken to emphasize on the impact this research can reach by developing a strong, durable, functional biomimetic robot. The biomimetics angle of our robot lies more in the goal of attaining the flexibility and strength of an octopus found in nature rather than mimicking its exact physiological mechanisms. Kraken weighs 9.52kg (20lb) with all its components, measures 0.5x0.25x0.25m (20x10x10in) in size and has 4 arms. We present the prototype design of the robot that is capable of operating underwater in a swimming pool 24x24x1.8m (80x80x6 ft). A hybrid actuation system is implemented to effectively actuate the octopus's arm to grasp objects underwater using stepper motors for three arms and TCP_{FL} for the fourth arm.
The TCP_{FL} are twisted and coiled polymer muscles constructed from fishing line. This actuator is based on previously presented work from our group, which focuses on the electrothermal actuation of the polymer-

based muscle (nylon 6,6) by integrating, through coiling, a heating wire (nichrome, 80 µm diameter) around the diameter of the polymer [9]. Our TCP_{FL} arm shows tremendous hope for the advancement in soft robotics as it occupies less physical space in the robot than other motors while still maintaining a considerable amount of strength for its size. The wireless configuration allows for increased maneuverability, especially in areas that exterior cables would otherwise become easily entangled in. Moreover, its smaller size would be beneficial for mobility in smaller spaces. A buoyancy system is implemented for vertical swimming of the robot. Having such a robot will help elevate the underwater research and exploration by making it more cost-effective, safe, flexible, and reliable.

The objective of this research is to create a wirelessly controlled, untethered octopus-like robot that is capable of grasping objects underwater using hybrid actuation methods, namely a combination of artificial muscles and stepper motors. This initial multi-system hybrid design focuses on the mechanisms of the designed silicone arms. The stepper motor system would serve as an example of showing the different bending options obtained from different stiffness options while the TCP_{FL} shows the potential of a new actuator that can perform similar functionalities of that of a stepper motor while still maintaining a low cost, highly flexible, and light weight system. The other objective is to be able to perform vertical swimming using the on-board buoyancy system, and identify the relationships of the input and output parameters.

Our design of the robot is robust and consists of:

- A 3-D printed dome-like exterior that has a watertight seal over all the electronics and hardware of the robot as shown in **Fig.1**. It has three layers, which are the actuation unit, buoyancy unit, and electronics unit.
- Six different soft flexible arm configurations offering multi-dimensional actuation options for grasping several objects shown in **Fig.2**.
- A hybrid actuation technology is presented allowing for each of the soft silicone arms to be actuated using a stepper motor or a TCP_{FL} actuator (**Fig.4).**
- The inexpensive TCP_{FL} actuators have high actuation (up to 50% strain), moderate stress (> 1 MPa), are easy to fabricate in house, can conform to geometries and therefore suitable to use in bioinspired robots.
- A buoyancy system consisting of an air bladder and CO_2 gas supply, valves are included in the robot, which allows vertical swimming underwater upon inflation and deflation.
- A wireless joystick controller allows for complete hands-off control of the robot's lithium-ion battery powered electronic subsystems as shown in the field test conducted in **Fig.1** and **Fig.5.**

1.1.Related Works

Underwater robots play a vital role in many exploratory expeditions. Many oceanic researchers and archeologists use robots to study deep water conditions (+1,000 ft), animals, and sunken histories. These robots can reach depths, withstand cold and harsh underwater temperatures (4°C to 1°C), and general conditions that a human is physically incapable of facing safely. In this regards, a unique robotic fish was developed at MIT based on a biomimetic fish. The fish is equipped with a camera which allows for the recording of aquatic life in their natural habitat [24]. Another fish was developed at Corporacion Universitario de Huila in Colombia that utilizes SMA wires for swimming [25]. A robotic jellyfish, Robojelly, was fabricated mimicking the features of the Aurelia Aurita jellyfish species that is actuated using shape memory alloys at Virginia Tech [26]. Later on, a fuel powered muscle consisting of nickel–titanium, multiwall carbon nanotube, and nano-platinum (NiTi/MWCNT/Pt) composite actuators [27] was proposed for the jellyfish-like robot. Free-swimming jellyfish like robot was shown recently by Frames et al. [28] from Florida Atlantic University (FAU) using hydraulic actuation system. They showed excellent untethered operation in the ocean and passing through a narrow obstacles. An inflatable soft pneumatic composite (SPC) actuators based jellyfish with payload was shown by Joshi et al.[29] from UTD recently. There many works in this area of biomimetics. An earthworm soft robot is presented from the University of Southern California that is capable of moving on both horizontal and inclined surfaces [30]. Researchers from FAU have also presented KnifeBot. An underwater vessel that is capable of multidirectional maneuvering from an integrated undulating fin [31]. An octopus found in nature can conform to many non-uniform shapes underwater, as its body is able to bend and flex in many degrees of freedom. The flexibility of its body also serves as a protective measure against predators. The octopus can bend and extend its arms, allowing it to easily maneuver on the sand at the bottom surface of the ocean [32]. The swimming maneuvers of an octopus consists of two steps. The first one is when the arms are spread apart (open, recovery stroke). The second is when the arms are quickly moved to close (power stroke). The power stroke allows for significant thrust, allowing the octopus to propel its body forward [33]. Some dynamic models of an octopus robotic system has been presented in [34,35]. Several studies can be found from the OCTOPUS Integrated Project funded by the European Commission. Among the prototypes presented, PoseiDrone, an octopus like robot shown in **Fig.S1(a)** (supplementary file), from The BioRobotics

Institute Scuola Superiore Sant'Anna Livorno, Italy, is made of several equidistant arms with swimming abilities imparted by using jet propulsion. Each arm has its own crank-like actuator that can bend or extend the arm using a sequence of sucking and releasing of the water from the chamber allowing for maneuvering [36,37]. An OctopusGripper, **Fig.S1(b),** is also presented by Festo Inc., with each gripper arm inspired by the shape of the octopus tentacle. They are made from a soft silicone elastomer, which is structured to control the bending direction using pneumatic actuators. The octopus-like tentacles of the OctopusGripper also contain suction abilities that can sustain a large gripping force with a working pressure of 2 bar [38]. A fully soft robot inspired by the octopus was presented by Fras et al. [39], seen in **Fig.S1(c)** with arms made of a novel soft fluidic actuator capable of manipulation as well as movement such as turning and forward propulsion. The robot is completely soft with even the main body being composed of an elastomer.

Calisti et al. [40] at the BioRobotics Institute in Italy has developed an octopus inspired robot. The concept presented contains a silicone arm with embedded cables that were actuated by servo motors to mimic the bending of the biological octopus tentacle. They have demonstrated the use of the arm by grasping objects and a pushing-based locomotion. Moreover, they have revealed the control of the arm stiffness by coiling and uncoiling of an embedded steel cable in the arm. Additionally, a multi-arm wirelessly controlled swimming octopus robot is presented by Sfakiotakis et al. from Greece [41,35,34,42], shown in S1(d). This robot was able to propel itself and swim in underwater at a speed of 0.26 body length/second driven by waterproof micro servomotors. It is also able to perform a turning maneuver using a sequence of actuation steps. The main body enclosure contains an empty cavity that can be filled with water, which is utilized to control the buoyancy of the robot. Moreover, a soft, robotic arm inspired by an octopus tentacle embedded with coiled SMAs is presented from The BioRobotics Institute. The arm can bend and manipulate objects, shown in S1(e). The arm is made of transverse coiled SMA muscles around a cylinder shape of the octopus arm [43,44]. An 8-arm octopus-like robot was fabricated and is seen in S1(f). This robot has 8 soft, silicone arms and a rigid central housing for a controlling unit. The neutrally buoyant robot was able to move underwater over different surfaces and physical constraints. It is also able to grasp objects of different shapes and sizes. The swimming and grasping are a result of using two different arm actuating units, the motor crank for locomotion and the coiled SMA technology for manipulation [45]. A case study has been presented which introduces the control of the morphology of an octopus arm [46]. A review paper presented by Kwak and Bae explored the possibility of utilizing the biomimetics of arthropods for underwater application. Salazar et al.[47,48] from New Mexico state University has shown the review of underwater robots and extensive literature. Table 1 show a brief comparison of Kraken and other fully developed octopus-like robots.

Key aspects of the robots are compared such as actuation technology used, type of locomotion, type of control, biomimetic structure, overall dimensions, and the resulting manipulation capabilities. The unique combination of technologies, both novel and traditional used in our robot, makes it an ideal underwater preliminary probe capable of adapting easily to different situations and gathering valuable data before a more complete solution is determined. **Fig.1(b)** shows Kraken deployed in the water (shown in movie 1, supplementary file). **Fig.1(c-d)** shows the octopus robot underwater and octopi found in nature with similar curling arm actuation. **Fig.1(e-f)** show the different grasping angles of the arm actuating and utilizing the hybrid system. We have shown controlling Kraken wirelessly in underwater conditions up to a depth of 6 feet (1.8m) shown in movie 2 and 3. Kraken is equipped with several arm stiffness configurations, which allows for the grasping of different object, shapes, and orientations (shown in movie 4). The new technology of twisted and coiled polymer actuators is used in one of its tentacles for grasping underwater. This was done to compare and contrast as well as identify the basic characteristics of the two actuation systems in underwater conditions, because we don't know the behavior of the TCP embedded arm motion in response to different input conditions and geometry. Therefore, experiments are necessary to determine those variables and identify the basic science of actuation such as fluid mechanics, heat transfer kinetics and manipulation associated with the motion of the arms. The results presented are explained in different sections. First, we present different stiffness configurations for the silicone tentacle. Second, a characterization of the performance of the TCP_{FL} actuator is presented. Then, we show the implementation of the TCP_{FL} arm in air and in underwater conditions. Next, we show Kraken deployed in a swimming pool highlighting its wireless capabilities and onboard controlling system. Kraken can perform dexterous tasks such as grasping and vertical swimming (shown in movie 2 and 3, supplementary file). Finally, we show flow analysis test results that were conducted to verify the design constraints and parameters of the robot.

Table 1: Comparison of current full octopus-like robots				
Name/ Category	Kraken (this paper)	PoseiDrone [36]	Octopus Inspired Multi-Arm Robotic Swimmer [42,34,35,41]	The Soft Eight-Arm OCTOPUS Robot [45]
Actuation Technology	• Stepper motors with tendon • Twisted and coiled fishing line actuator TCP_{FL}	• Dyneema cables drivin by servomotors	• Servomotors Hitech, HS 5086WP	• Motor driven tendons • Coiled shape memory alloys
Locomotion/ propulsion	• Vertical swimming using buoyancy system	• Crawling by pushing and pulling. • Swimming using a buoyancy module and pulsed jet.	• Swimming and turning using the movement of its arms.	• Able to crawl using push and pull strategies
Control	• Wirelessly controlled	• Controlled externally through a connecting wire.	• Controlled remotely through an RF connection.	• External communication
Sensors	• Temperature	• None	• None	• Contact sensors • Stretch sensors
Structure	• 3D printed housing composed of 3 levels • 4 soft silicone arms mounted on bottom level.	• Composed of six arms, a swimmer module and a buoyancy module.	• Eight compliant arms mounted to a compliant housing with buoyancy and electronic systems.	• Eight arms mounted to a platform on which the motors are mounted.
Dimensions	• Weighs 9.52 kg • Arm length 0.25m • Size 0.5x0.25x0.25 m	• 0.78 m long • 0.245 m/per arm	• 0.2m arm length • 0.16m radius • Weighs 2.68 kg	• Arm length 0.3m
Manipulation	• Capable of grasping using stepper motor arms • Lifting weights using the TCP_{FL} arms	• Able to lift and hold items while moving.	• Able to grasp using multiple arms	• Two arms using SMA.
Powering / duration	• Lithium ion battery 4400 mAh. • 45 minutes swimming	• None	• Li-Po battery • 1 hour continuous operation	• None

2. Materials and Methods

As stated earlier, the objective of this research is to create a wirelessly controlled untethered octopus-like robot using a combination of artificial muscles and stepper motors. Here, we describe the materials used and the testing methods in both experimental and theoretical frameworks.

2.1. Twisted and coiled polymer (TCP_{FL}) fishing line actuator

Artificial muscles such as TCP_{FL} can be controlled either by hydrothermal actuation or joule heating. In our case, Joule heating is the most ideal, as it eliminates the necessity to add complex water heating and cooling systems within the octopus robot structure. To introduce Joule heating into a material that is inherently nonconductive, several researchers have introduced electrical wires such as copper wires [49], and flexible carbon nano tubes sheets on to the twisted coils [1]. Wu et al [9], from our group, has introduced a novel method of wrapping nichrome resistance wire on to the fishing line fiber after twisting and before coiling. This specific method allows for the use of thin nichrome wire of 80µm diameter.

The small diameter has a minimal effect on the coiling process during fabrication as well as the mechanical performance of the actuator. Also, the thin wire allows for a more uniform and condensed temperature gradient throughout the muscle when heating. This ensures an even distribution of the temperature. We have followed very similar fabrication methods to our previous work presented in [6] to achieve high quality data on the actuator used in the robot arms. However, we created self-coiled structures that have high forces in this study.

The complete properties of the actuator are found in **Table 2**. The TCP_{FL} has an actuation strain up to 40% using an electrothermal mode of actuation.

2.2. Fabrication of fishing line muscle with thin heating wire

The fabrication of the self-coiled fishing line muscle with heating element is simple, scalable, and easy to follow which allows for in-house manufacturing of the actuators at low cost. It consists of four major steps following Wu et al. [9] and shown in movie 9, explained in **Fig.S2** [9]. First, twist insertion; second, wrapping of nichrome resistance wire; third, coiling; and fourth, thermal annealing and training. We used a precursor fiber of fishing line muscle, purchased from Eagle Claw (0.8 mm in diameter and 1143 mm in length), to a motor (mounted on the top) and the other end to a 500g deadweight. The precursor fiber is twisted and then nichrome wire is incorporated as a heating element. This process is important to avoid breakage of the thin wire (80 µm). After that, the muscle is coiled; it is crimped on both ends and annealed in a furnace at 180°C for 90 minutes to preserve its coiled shape. This annealing process aligns the crystal structure of the nylon, which allows it to stay at the coiled shape. **Fig.1 (a)** shows the self-coiled fishing line muscle after annealing with diameter D = 2.80 mm. Lastly, the muscle is trained at multiple heating cycles at 300g load following the protocol shown in **Fig.S2 (c)** to retain a certain actuation load. Thermal imaging of before (t = 0s) and during actuation (t = 5s) is shown in **Fig.S2(b).** Note that all supporting information and figures are provided in supplementary files and they are designed with "S" to differentiate with the main figures.

Table 2: Fishing line TCP actuator information

Material	Nylon (6,6) fishing line
Type of actuation	Electrothermal
Type of resistance wire	Nichrome (nickel, chromium)
Resistance wire diameter	d_w=80 µm
Precursor fiber diameter	d =0.8 mm
Length of precursor fiber	l = 1143 mm
Weight for fabrication	m_f = 500 g
Annealing Temperature/ Time	Ta=180^{0}C/ 90 min
Training protocol	According to figure 5 (c)
Diameter after coiling	D=2.8mm
Length after coiling	L=110 mm
Resistance	R= 256Ω
Current (Input)	I= 0.14A - 0.47A
Voltage (across the actuator)	V= 35V - 120V
Input power (V*I)	P = 4.9W - 56.4W
Heating time(t_h)	t_h=25s - 1s
Cooling time (t_c)	t_c =100s - 9s
Heating energy($V*I*t_h$)	E_h=122.5J - 56.4J
Actuation frequency	f = 8mHz – 0.1Hz
Actuation strain, at 300g load	ε = 40% - 10% @3N load
Blocking force (experimental)	~5N (500g)

2.3. Isotonic testing of fishing line muscle

Isotonic testing of the actuator was done by hanging a calibrated weight (constant load) at the tip of the actuator and taking measurements of the, voltage, current, temperature, and displacement. A square wave current input was applied to the muscle while data, such as performance under actuation strain, temperature, and output voltage were collected and analyzed. **Fig. 3(a)** shows the schematics of the experimental setup. The set up contained the fishing line actuators, NI DAQ 9219, Keyence laser displacement sensor, thermocouples, LabVIEW program, power supply, and calibrated weights. **Fig.S3(a-c)** show the connection circuit. The test was conducted at three different current inputs of 0.2A, 0.3A, and 0.4A.

2.4. Overall robot design and manufacturing (mechanical and electrical components)

The novel robot is divided into three levels. The first level contains the four 5.5 kg-cm bipolar NEMA 17 stepper motors and the TCP_{FL} actuator that control the soft silicone arms. The second level contains the buoyancy system, which is comprised of two solenoid valves, check valve, pressure regulator, air bladder, and a 16g CO_2 canister. Lastly, the third level contains the electrical controlling circuit, which includes the wireless communication module, a battery power source, an Arduino board, a voltage boost converter, and motor drivers. The overall sealing process is one of the most important processes for the underwater robot. We used Flex Seal Paint™, Flex Seal Tape™ and silicone EcoFlex 00-35 to seal the casing of the octopus robot (**Fig.S4, S5,** and **S6**).

A wireless joystick controller for a user interface, **Fig. S6,** was created to wirelessly control the robot up to 25ft. The program allows a user to select and activate each task, one at a time. The main menu selection starts by selecting between arms 1-4 or the buoyancy system. If an arm is chosen, the user can push up or down to actuate it to either grab or release an object. If the buoyancy system is chosen, the user can inflate or deflate the air bladder to control the vertical depth of the Kraken.

2.5. Flow Simulation

An underwater flow simulation study of the vertical motion of our robot is studied using ANSYS Fluent (v17.0) software and the analysis is a transient incompressible flow analysis. Yue et. al [50] suggests simplifying the 3D model so as to reduce the computational time and get more effective results for this type of underwater studies. In our case, the model is split vertically in half in order to dimensionally reduce the domain. The mid-plane is assigned the symmetry boundary conditions while the sides of the domain are assigned as walls. The pressure is assumed constant throughout the domain because of the relatively small difference in vertical height. In order to impart the motion, a user-defined function is compiled in Fluent. The user-defined function consists of the physical properties of the robot. The surface of Kraken is assigned the wall boundary condition $U\text{-}U_{wall} = 0$

Two flow simulations were done. First, moving the model vertically upwards with a velocity of 1 m/s for 1s, giving it a Reynolds' number of around 5.7e5. Second, letting it sink under acceleration of 0.0198 m/s^2 for 8s, which is calculated from the experiment (time-dependent velocity). Two methods can be used to define the interaction between the model and the fluid: (a) dynamic meshing, which sets the fluid as stationary and the model to move, and (b) fluid moving in the opposite direction as the model, which mimics the relative motion between the two [50]. Both these methods were analyzed by Leong et al. [51] who concluded that the results provided by both of them are just marginally different from the experimental results. A detailed description of the ANSYS Fluent simulation procedure and parameters are documented in the supplementary file (**Fig.S7**).

3. Results

We first started by conceptualizing the octopus-like robot to have a modular and multilayered structure. After the CAD design was completed, we fabricated the robot using an additive manufacturing method using 3D printing. The assembly was built to create the final structure with all its electrical and mechanical components. The robot weighs 9.52 kg with all its components and measures 0.5x0.25x0.25m in size. The rigid robotic structure is 3D printed using ABS material. The robot is composed of three levels as seen in **Fig.1(A)** with the first level containing the mechanical actuation components. The second level contains the buoyancy system, and the third level contains the controlling circuit. **Fig.1(A)** shows zoomed in photo of the TCP_{FL} actuator used in the arm. Kraken can function underwater for 45 minutes using a lithium ion battery with a capacity of 4400 mAh. Vertical swimming is achieved with the equipped buoyancy system, and grasping is achieved with the four silicone arms. Three of the arms are actuated using stepper motors and the fourth arm is actuated using TCP_{FL} actuator powered by a circuit and a battery. The TCP_{FL} arm also contains an embedded temperature sensor that can monitor the performance of the artificial muscle. Kraken was tested in both a lab setting using a 70-gallon fish tank to test the TCP_{FL} arm, and in an Olympic size swimming pool using the stepper motor arms to quantify and show the grasping performance of the robot using both actuation technologies. The summary of the test results is described quantitatively and qualitatively as follows:

- Six different soft flexible arm configurations offering multi-dimensional actuation options for grasping several objects shown in **Fig.2**. The TCP_{FL} actuated arm presented with up to 40^0 bending using 0.0508 mm (0.002 in) thick spring steels embedded in a 3 mm thick silicone.
- Characterization of the robot arm showing up to 40° bending in air conditions and 21° bending in underwater conditions using novel TCP actuation technology (**Fig.4**).
- Grasping underwater utilizing TCP actuator and stepper motors.
- Vertical swimming using the on-board buoyancy system and testing in a swimming pool of depths up to 6ft (**Fig.1**and **4**).
- Wireless controlling capabilities for both the stepper motor and the TCP_{FL} actuator (**Fig.1** &**4**).
- Flow simulation of the octopus robot sinking and floating (**Fig.5**).

3.1. Silicone arm configuration

One of the important parts of the robot is the flexible arm that is used for grasping different objects. To this end, we explored different arm stiffness. Six different stiffness configurations are presented in **Fig.2(a-f)**. The variable arm stiffnesses are achieved by embedding different shapes and layouts of the spring steels, thickness of 0.003in (76µm), in the silicone as seen in **Fig.2(g)** during molding**.** The layout parameters, shown in **Fig.2(h)**, include changing the number of spring steels, embedded length (L), thickness (t), and number of springs (n). **Fig.2** shows six different bending configurations according to the spring steel layout presented on the left. 2D bending on the XY plane is achieved as shown in **Fig.2 (c and e),** while 3D curling is achieved as shown in **Fig.2(a, b, d, and f).** The Kraken arms can be easily interchangeable by sliding them into the 3D printed arm lip and fastening using a hose clamp. The variability of the arm stiffness is dependent on the object it is aiming to grab. **Fig.2(i)** shows different silicone arm stiffness configurations attached to the base structure

of the robot. The different geometry and topology of the soft silicone, and the hard very thin spring steel enables the arms to actuate in different modes of actuation. Each arm mounted in the robot (shown in **Fig.2(i)**) are different, making the robot unique and capable of handling different tasks. Different configurations are shown in movie 4. All the arms can be made with the same stiffness materials but that will limit the capability of the robot handling different objects. One basic scientific question we tried to answer in this case is, how the actuation of the arm is influenced when the geometry and the materials are varied. Here, we showed that in order to have a curling or bending actuation, like that of the natural octopus, it is not necessary to have a similar muscular hydrostat with so many radial and longitudinal muscles, instead one actuator, namely a very thin, 76µm spring steel and 3mm silicone elastomer is enough for the arms to exhibit different motions that are essential for grasping objects.

3.2. TCP_{FL} isotonic testing

Testing of the novel actuator twisted and coiled polymer based on fishing line (TCP_{FL}) is essential to understanding its performance in various scenarios. The basic questions are: What is the behavior of the TCP actuator when embedded in the silicone arm? What are the parameters that affect the performance of the embedded systems? There are limited studies available when it comes to TCP embedded in silicone elastomers [3]. Therefore, experiments are necessary for the TCPs, as well as when embedded within silicone and making the arms of our robot. First, experimental characterization was performed on the self-coiled fishing line actuator (loaded length L=120 mm, diameter D = 2.8mm, resistance R = 312 Ω) without embedding in silicone. The photograph of the experimental set up and schematic diagram are shown in **Fig.3(a,b)**. The testing setup and experimental conditions are explained in detail in the *materials and methods* section and the supplementary document. A constant load of 300g was applied as a pre-stress parameter to the actuator because the maximum actuation stroke for fast actuation (2s ON and 50s OFF, 0.4A) is at this load. **Fig.3(c-e)** shows cyclic actuation strain, temperature, and power (2s ON and 50s OFF) for three input electrical current magnitudes. The actuator produces an amplitude strain of ~ 20% at 0.4A. **Fig.3(f-k)** show experimental results on the effect of input energy (heating time, voltage, and current) on the actuation performance (stroke %) and temperature change while still maintaining a constant cooling time of 50s**. Fig.3(f,g)** are results for 0.2A input current with the variation of heating time from 2s to 7s, where an increase of 13% in the actuation strain is observed**. Fig.3(h,i)** are for 0.3A input current and variation of the heating from 2s to 4s, which shows an increase of almost 20% actuation strain. Likewise, **Fig.3(j,k)** are for 0.4A current with heating times of 1s and 2s, an increase of 13% is also observed. The results show that the increase of input energy will significantly increase the performance of the actuator. The input energy is the product of power and heating time. An average of 20% strain is achieved at a temperature of 100^0C for all 3-current magnitudes with varying energy consumptions.

3.3. TCP_{FL} embedded in the arm and tested in a fish tank

The second set of experiments was the actuator in embedded conditions. We present the TCP_{FL} actuator with a length of 100 mm (R = 335 Ω, pre-stress at 300g loading conditions) embedded in one of the silicone arms and tested in both air and underwater using a 70-gallon fish tank in a lab setting (the air test was at room temperature, the water temperature was 21°C). The experimental set up is shown in the schematics in S3(a,b). **Fig.4(a and b)** show the schematic diagram and photograph of the actuator embedded in the arm showing the bending angle. The silicone arm triggered by the TCP_{FL} actuator shows a good potential for grasping due to its high bending angle. **Fig.4(c)** shows the effect of input current on the bending angle for the actuation in air medium and in underwater conditions respectively. When tested in air, an increase in current increases the bending actuation in a non-linear fashion except a slight decrease when the current is 0.2A for all heating time (10, 15 and 20 s). This could be due to the heat trapped within the silicone, which prevents further actuation. In water, the trend is slightly different. Overall, the increase of energy results in an increase in bending. **Fig.4(c)** shows that the bending angle in air and in underwater is almost doubled when the energy is doubled. This can be clearly seen in the underwater bending results. For example, at 0.2A with 10s and 20s heating the power consumption is ~13W ($P = R*I^2$, assuming constant resistance) the energy would be 130J and 260J respectively which results in an increase of bending angle from 10^o to 20^o. **Fig.4(d)** shows results for the bending angle vs. time for both in air and underwater conditions. In air, the arm can bend up to a maximum of 38° from its original position at an input current of 0.16A for 20s heating (output voltage is 54V). In water, it can bend up to 21° using the same energy consumption. **Fig.4(e)** presents cyclic actuation results in underwater conditions. Here, it is also observed that the higher bending angles are produced at higher energy values with continuous heating. Movie 5 and movie 6 show the arm actuating in underwater conditions. **Fig.5(f-h)** presents the TCP_{FL} arm lifting several objects that are anchored using a string at the tip. The arm can lift objects such as PVC pipe and calibrated weights. Movie 7 shows the fishing line arm capable of lifting several objects underwater. Due to the large voltage required to actuate the TCP_{FL} actuators, in order to

wirelessly control the actuator using a battery, a step up voltage converter was added to the controlling circuit as shown in **Fig.S7 (a).** This circuit is capable of increasing the voltage from 14.8V up to 130V which is more than sufficient to provide the voltage needed to use the TCP_{FL} at its maximum performance.

3.4.Testing underwater in a swimming pool using the stepper motors

The third set of experiments was a field test of the robot to show robustness of the design. Kraken is completely functional when submerged underwater, as shown in supplementary movie 1and **Fig.S8**. Utilizing the stepper motors, it is fully capable of grasping objects such as a small PVC pipe using an octopus-like, flexible grabbing motion. Testing in the swimming pool was conducted using the stepper motors powered by an onboard Li-ion battery as the primary source of arm actuation. Grasping of a small PVC pipe can be observed in **Fig.4(i, j, and k)** and movie 2. A 2.5 kg weight is attached to the robot as shown in **Fig.4(l)**. Kraken is still able to float while carrying heavy loads as shown in **Fig.4(m)**. **Fig.4(n)** shows a snapshot of the octopus floating on the surface with silicone arms fully extended. **Fig.4(o)** shows an interesting configuration of 3 arms actuated at their different curling motions using the mode shown earlier in **Fig.2(c, d, and f)**. The ability to bend its arms according to the situation while maintaining a minimum size or profile is one unique feature of this robot. Moreover, vertical swimming while carrying a heavy load is presented. **Fig.4(p)** shows Kraken releasing air to sink to the bottom surface of the pool, also shown in the supplementary movie 3. Lastly, **Fig.4(q)** shows Kraken carrying both the heavy payload and grasping the PVC pipe.

3.5.Flow Simulation

To understand the fluid-structure relationship while the robot is moving, flow studies are performed here, keeping the solid model of the robot (see material and methods for the simulation procedure). Essentially, the fluid domain and rigid body are defined, the rigid body was subjected to have a velocity, and the pressure at the top and bottom was set to be zero, and the simulation was performed in ANSYS. The results show that the flow is only affected in the close vicinity of the rigid body motion of Kraken but the magnitude/pattern of curling, circulation and other properties are essential to understand the behavior. The streamlines propagate from the Kraken opposite to the direction of movement, leaving behind turbulent recirculation similar to what is expected from an underwater rigid motion. The rising up simulation is implemented at a much higher speed (1 m/s) and hence generates more recirculation as can be seen in **Fig.5 (a-d)** compared to recirculation while sinking is seen in **Fig.5 (e-h).** This can also be accounted for the fact that the wake surface has a sharp edge while rising, whereas the wake surface has a smoother surface transition while sinking. These results will be useful to determine the flow behavior of UUVs (unmanned underwater vehicles). The sinking acceleration is very small (~0.02 m/s^2, measured from experiment) due to buoyancy and viscous drag acting on the body. The wall shear (τ_{ij}) is calculated by equation (1) and the results are shown in **Fig.5 (i-k)** with the legend in the left side.

$$\tau_{ij} = \mu_i u_j + \mu_j u_i \tag{1}$$

μ_i and $\mu_j$are the dynamic viscosity in the x and y direction, and u_j and u_i instantaneous velocities in the y and x direction. The flow field resulting from the motion of Kraken is calculated by the unsteady incompressible Reynolds-averaged Navier Stokes (RANS) equations as shown in equation 2 and 3:

$$\frac{\partial u_j}{\partial x_j} = 0 \tag{2}$$

$$\frac{\partial u_i}{\partial t} + \frac{\partial u_i u_j}{\partial x_j} = -\frac{1}{\rho}\frac{\partial P}{\partial x_i} + \nu \frac{\partial}{\partial x_j}\left[\left(\frac{\partial u_i}{\partial x_j} + \frac{\partial u_j}{\partial x_i}\right)\right] - \frac{\partial \overline{u_i' u_j'}}{\partial x_j} \tag{3}$$

where u_i and u_i' are the mean and fluctuating components of the instantaneous velocity, P is the mean component of instantaneous pressure and ν is the kinematic viscosity. The realizable k- ε turbulence model with scalable wall functions solver is used to study the dynamics of the fluid domain.

4. Discussion

We presented the results of the Kraken in a swimming pool as part of a field test. Kraken could grasp objects such as a PVC pipe, float and sink with 2.5kg load mounted on its structure and achieved vertical swimming all wirelessly controlled by a joystick from a user standing outside the pool.

Experimental studies are presented for the TCP_{FL} used as an actuator embedded in the soft silicone (EcoFlex 00-30) in a lab setting. Different styles of arm configurations were studied. We found that the variable stiffness configurations are extremely beneficial to accommodate grasping of delicate and complex

shaped objects. Utilizing this technique, each arm mounted on the octopus-like robot can have a different stiffness option, which can widen the use of the grasping action underwater. These possibilities can be achieved using flexible and soft material, thin spring steel and one single actuator with a tendon. We answered the question of whether or not a few actuators are enough to mimic an octopus like robot arm for grasping objects. The six different arm configurations allow for a wide range of arm flexibility that can help divers and researches in underwater tasks such as holding equipment, samples, and interacting with live species delicately. Actuators fabricated from fishing line nylon 6 (TCP_{FL}) have been presented, which provide an actuation stroke of up to 20% and high pre-stress conditions (300g load), and the blocking force is greater than 400g (4N) when triggered with 0.4A current/~58V Voltage. We have presented the fabrication of a fishing line actuator using the self-coiled method, which is explained in detail in the materials and method section. This actuator is light in weight, flexible, inexpensive ($200/kg including nichrome); it can produce large actuator strain and is capable of carrying weights up to 520 times its own weight (TCP_{FL} 0.772g, can carry up to 400g). These properties make this actuator suitable for many bioinspired swarm robots, since we can make multiple robots without much material cost. For example, if SMAs are used, they cost $3000/kg compared to the cost of TCPs which is $200/kg. Experimental characterization of the fishing line actuator is presented in **Fig. 3.** Here, the actuator shows great performance under a 300g pre-stress condition.

The variation of input current and heating time is very critical due to the temperature sensitivity of the actuator. If the temperature exceeds its melting point 250°C when heating is applied, the muscle will burn and will no longer be able to actuate. Equation (4) can be used for the temperature prediction according to the electrical input to the actuator. Where $T(t)$ is the temperature of the actuator at time t, T_∞ is the ambient room temperature, R_o is the resistance of the actuator at room temperature, i is the input current, A is the cross-sectional area of the precursor fiber of the actuator (nylon), m is the mass of the actuator, c_p is specific heat, and α is the temperature coefficient for the resistivity.

$$T(t) = -\frac{R_o i^2}{-hA + R_o i^2 \alpha}\left(1 - e^{\frac{-hA+R_o i^2 \alpha}{mc_p} t}\right) + T_\infty \quad (4)$$

The resistance change is due to the temperature change [52], which is calculated using Equation (5).

$$R(t) = R_0[1 + \alpha(T(t) - T_\infty)] \quad (5)$$

The temperature coefficient of resistance of the nichrome wire is α = 5.78 x 10^{-4}/°C [53] and the ambient temperature T_∞ = ~23°C. We can predict the resistance change during actuation with respect to time. Equation (6) and (7) can be used to calculate the electrical power (P) and electrical energy (E) provided to the actuator, by adjusting the electrical current input (I), input voltage (V) and duration of input time (t).

$$P = I\,V \quad (6)$$
$$E = Pt = I\,Vt \quad (7)$$

By observing the actuation results for the TCP_{FL} from **Fig.3 (c, d, and e)**, we can see that the actuation stroke is very much dependent on the input current (Δ=0.1A difference), the time the current is applied (an order of 1s to 7s), and the pre-stress of the actuator (50-400g). Equation (6) and (7) can be used to calculate the energy consumed which is shown to affect the actuation performance of the TCP_{FL}. We noted earlier that in all three cases in **Fig3.(g-l)** almost 13% strain increase is achieved at higher energy values. Considering, **Fig.3 (e)** (input power at different current magnitudes), and **Fig.3 (f)** (The actuation strain at 0.2 A, for 2 s and 7s), the input energy is E = 15Wx 2s = 30J for the 2 second heating. Similarly, for 7 seconds heating, E = 15Wx 7s= 105J. Therefore, we can say that the increase of energy from 30J to 105J results in 13% actuation strain increase. Similar properties are observed for the other plots for **Fig.3 (h and i).** The cooling cycle also has an effect in the displacement of the actuator, which is visible in the cooling cycle, showing exponential decay. A bias is observed in the actuation strain at 50s (when the first cycle is finished), which is an indication that higher cooling times are needed to decrease the bias. In our robotic application, an increase in the heating time is needed in order to help the arm achieve higher bending angles and to tightly curl the arm after running for a few cycles. However, this will result in low frequency. Some of the drawbacks of this actuator are the low frequency (below 7 Hz [1]) and low efficiency (below 1%), but the contractile efficiency per weight of the actuator is 12.64%/kg. The efficiency is the ratio of the energy output to the electrical input energy. It is noted that the efficiency of TCPs is the same order as the efficiency of SMA actuators, which has been in research for the last 60 years. The TCPs are relatively new, 5 years since their introduction to the scientific community, and therefore, more needs to be done to improve them. There are some solutions to improve the performance in energy efficiency and actuation such as pulsed actuation [5], active cooling [54,55], and a locking

mechanism [11] can be used to improve the efficiency, conserve energy and increase the frequency. Nevertheless, the advantages of this actuator are that it is inexpensive, ideal for swarm systems and they are lightweight.

After implementing the actuator in the silicone arm (configuration 5, **Fig.2(f)**) at pre-stress of 3N, the test results showed that the arm could achieve a maximum of the 40° bending angle in air medium (**Fig.4 (d)**), compared to the 21° angle in underwater conditions at the same input current and heating time (**Fig. 4 (e)**). The decrease in the bending angle in underwater medium is due to several factors. First, the cold temperature of the water prevented the actuator from reaching its optimal temperature for maximum bending, which is why increasing the heating time was necessary during experiments. This is related to the convective and conductive heat transfer process, which needs further study via modeling and simulation. Second, while actuating in air medium, the arm is faced with minimal external forces. But, while actuating in underwater conditions, the arm is subjected to external forces (distributed pressure load) such as the pressure due to depth and flow of the water. Multiple actuators can be added in parallel in each arm in order to enhance the grasping performance of the silicone arms. Moreover, a locking mechanism can be implemented to achieve tasks such as grabbing and holding. These would be beneficial for applications related to underwater data sampling.

We had first showed the characteristics of the fishing line actuated arm under various power and frequency conditions in underwater. We have then showed the TCP_{FL} line functioning wirelessly using its own circuit in the fish tank. Future work will focus on the full integration and field testing for the system as a whole. If we use TCP_{FL} for each arm entirely, the space usage will be minimized to be even smaller and will make the robot more biomimetic due to muscle-like actuation. In addition, it increases the efficiency of its wireless capabilities, which will further reduce its cost and overall be a good choice for aquatic robotic research. Kraken has a lot of potential in assisting in underwater endeavors, such as replacing remotely operated vehicles and assisting in underwater explorations, pipe opening/closing and cleanups. It can also save lives in a swimming pool or the ocean when a camera is mounted in the body and it may be able to pull a victim out of water using artificial intelligence, when it is fully developed. The stress simulation results in **Fig.S9** in the supplementary show that the cage with carbon fiber material would be structurally safe to operate at depths up to 100 ft under stress of 60 MPa (3.02 atm pressure). The flow simulation model (**Fig.6**) can help in studying different designs of Kraken computationally, which can save time and resources spent on experimental studies. These design iterations can include different structures, masses, and fluids at various depths in which Kraken is deployed. The turbulent model can provide accurate and superior performance in flows involving recirculation [56]. The surrounding pressure is not affected much with time since the speed gained by the body is very small to cause considerable flow separation as shown in **Fig.5 (i-k).** The velocity contour is consistent with the one shown by Yue et al. [45], the only difference being that Yue et al. [45] has a stationary body and moving fluid, while our model has stationary fluid and moving body. The wall shear contour obtained corresponds to the profiles shown by Wang et al. [57], Zhang et al. [58], and Zhou et al. [59] for their respective underwater simulations. More studies can be done on the recirculation generated if they can be helpful for other things such as energy harvesting. This new robot has the capability of opening new doors in underwater exploration and can lead to new discoveries and understanding the world beneath our waters.

5. Conclusion and Future Work

In this paper, we presented a novel octopus-like robot known as Kraken that is actuated by a hybrid system consisting of stepper motors and artificial muscles. The robot has four different flexible arms that allows grasping of objects in different modalities. We showed experimental results of the robot deployed in a swimming pool as shown in **Fig.1 (b, c, e, f)** and in movie 8, a summary of important aspects of the robot is presented in table 1. There have been some octopus-like robots shown in the literature that have gripper arms but do not swim, others that are only capable of swimming, and others that are capable of both swimming as well as grasping. Significant data and experimental results have been generated from other research groups, which helped the current study. Unlike what we presented, most of the robots in the literature lack one or more features such as the variability or arm stiffness, or multimodal bending. Most of them do not include an onboard buoyancy system, powering means or untethered operation. Our robot utilized a combined actuation system of both stepper motors and artificial fishing line TCP_{FL} actuators. The robot is wirelessly controlled through a communication between the onboard controlling circuit and the wireless joystick used by the user at distances up to 25 ft. The robot can operate up to 45 minutes using the onboard lithium ion battery. The mounted buoyancy system in level 2 allows Kraken to swim vertically at various depths (tested in a 6ft deep swimming pool).

We have presented different arm configuration in **Fig.2** (movie 4) that can produce variable bending capabilities of the arm. The flexible arms actuated have different configurations tailored to grasp various objects underwater. The variability of bending will help in accommodating the different objects. We also present a novel actuation method that is used for grasping. This inexpensive novel actuator offers an actuation stroke up to 20% at 3N load. The TCP_{FL} actuators were extensively characterized to understand the physics of

the actuator (**Fig.3 & Fig.4**), and we showed excellent bending of the robot's arm. The actuator is significantly smaller and lighter than the stepper motors allowing for further advancement in optimizing the size and shape of the robot that is inspired by nature. The hybrid system was tested in both a lab setting (TCP arm, movie 5, 6, 7) and in a swimming pool (stepper motor arms, movie 1, 2, 3, 8), **Fig.4**. In order to study the fluid structure relationships and flow behavior of the robot, simulations were carried out and analyzed.

Future work will include developing a custom-made controlling circuit, analytical modeling and control algorithms. Optimized mechanical design of the robot include material choice and structural arrangement. Further testing should be done using other types of silicone elastomers, stiffness control, and actuation parameters to determine an optimized octopi's structure for oceanic exploration. Due to the power and battery limitations, the integration of a voltage boost converter to the circuit is essential in making the robot fully dependent on the actuation of the fishing line muscle for grasping. We have shown the actuating circuit (**Fig. S6**) for both the stepper motors and the TCP_{FL} using the boost converter to increase the voltage provided by the battery by decreasing the current output. Due to the actuator's high resistance (R= ~200-400 **Ω**) it takes low current (I = 0.12A-0.5A) but high voltage (V= 30V-150V), therefore, stepping down the current creates no issues for this application. We will combine the circuit and make custom made PCB in the future.

When developed further, it would be feasible for the TCP actuators to replace the stepper motors and reduce the space needed for actuation and increase the room for other sensory equipment such as cameras, chemical sensors, seismographs or other equipment useful in exploration that would previously require a much larger robot. Extensive studies of the TCP_{FL} polymer muscles that were embedded in the silicone elastomer for use in underwater grasping will help other researchers to use the data and create similar robots. We identified the bending mechanics and the heat transfer mechanism of the muscles for correlating the basic physics for underwater application. We also performed fluid-structure simulation studies to understand the motion and flow behavior of the robot during swimming. The implementation of the TCP_{FL} in the robot serves as a mechanism to maintain the flexibility of the arm while minimizing the space taken by the actuator. Due to the size of the robot as well as the minimal impact it makes in terms of noise and vibrations of the TCP_{FL} actuator, the robot can serve as an exploratory tool in situations where minimal interference is necessary. Typical mission-specific scenarios may require a delicate touch where noise and vibrations would alert other life. We observed that the stepper motors have some noise during underwater testing, which should not be ignored. Meanwhile, the flexibility of the arms, when developed further, will allow the robot to grasp objects when space is limited. This will lead to a higher adaptability when dealing with situations where space will be an issue, such as crevices. We hope that the results presented can be a stepping-stone in improving underwater robots and can be relevant to other researchers who would like to mimic the structure. It should be noted that we did not attempt to mimic the entire structure of an octopus arm that has complex muscle arrangements, suction cups, and a deformable body structure (the mantle), we only took a few of the important structures and demonstrated a fully functional field robot that can assist human being in different scenarios as shown in movie 8 where some of the authors were directly interacting with the robot underwater.

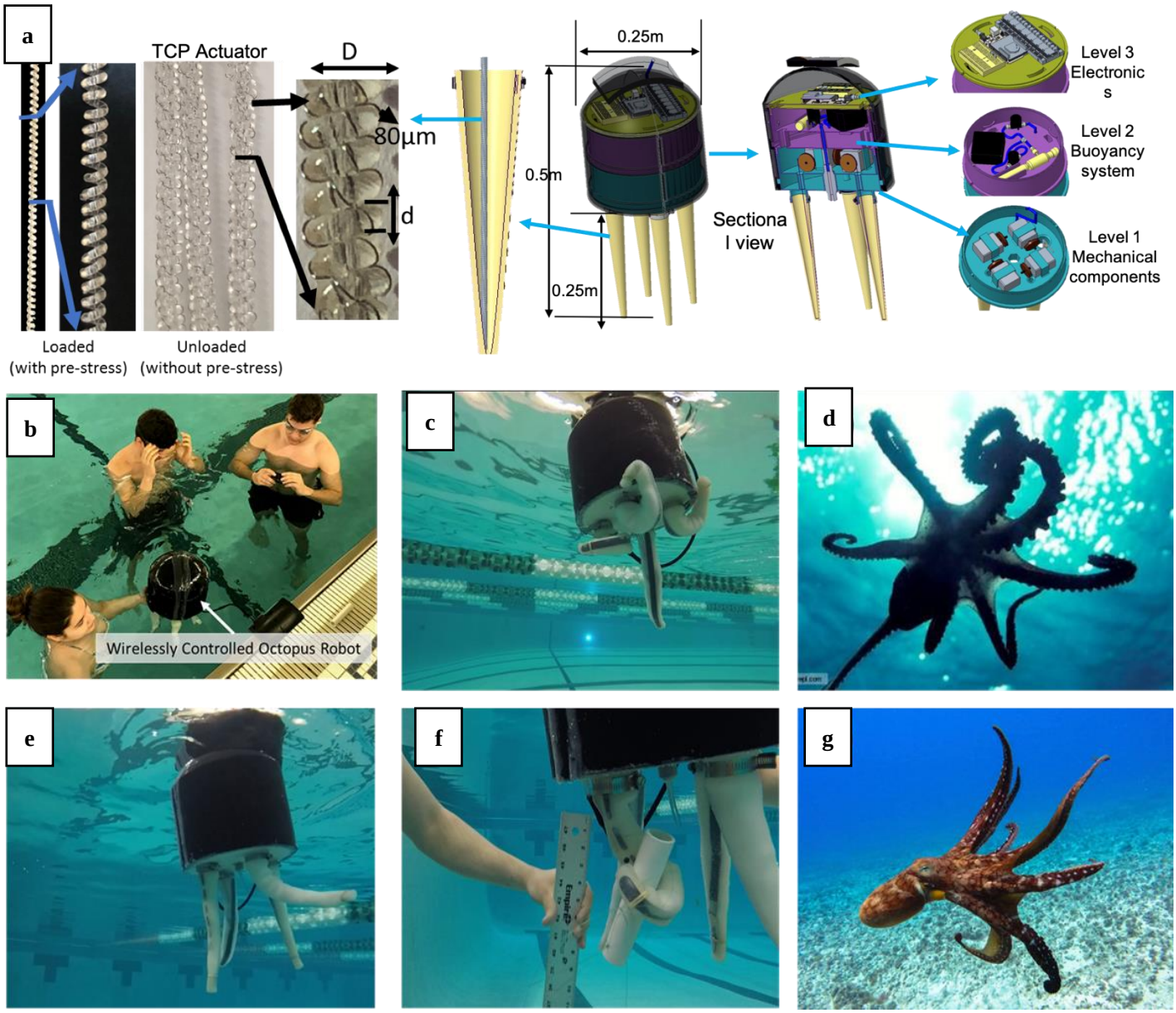

Fig. 1: Kraken hybrid robot for underwater grasping. (a) TCP fishing line actuator in loaded and unloaded conditions after annealing, diameter *D* = 2.80mm. The type of resistance wire is: Nichrome (nickel and chromium) with diameter d_w=80 µm. CAD schematic showing the major components of the hybrid robot where level 1: the mechanical actuation unit, level 2: the buoyancy system, and level 3: the controlling circuit. (b) Kraken deployed in water. (c) Curling 3 arms. (d) Octopus found in nature with curling arms. (e) Floating on the surface. (f) Grasping PVC pipe underwater. (g) Natural octopus swimming.

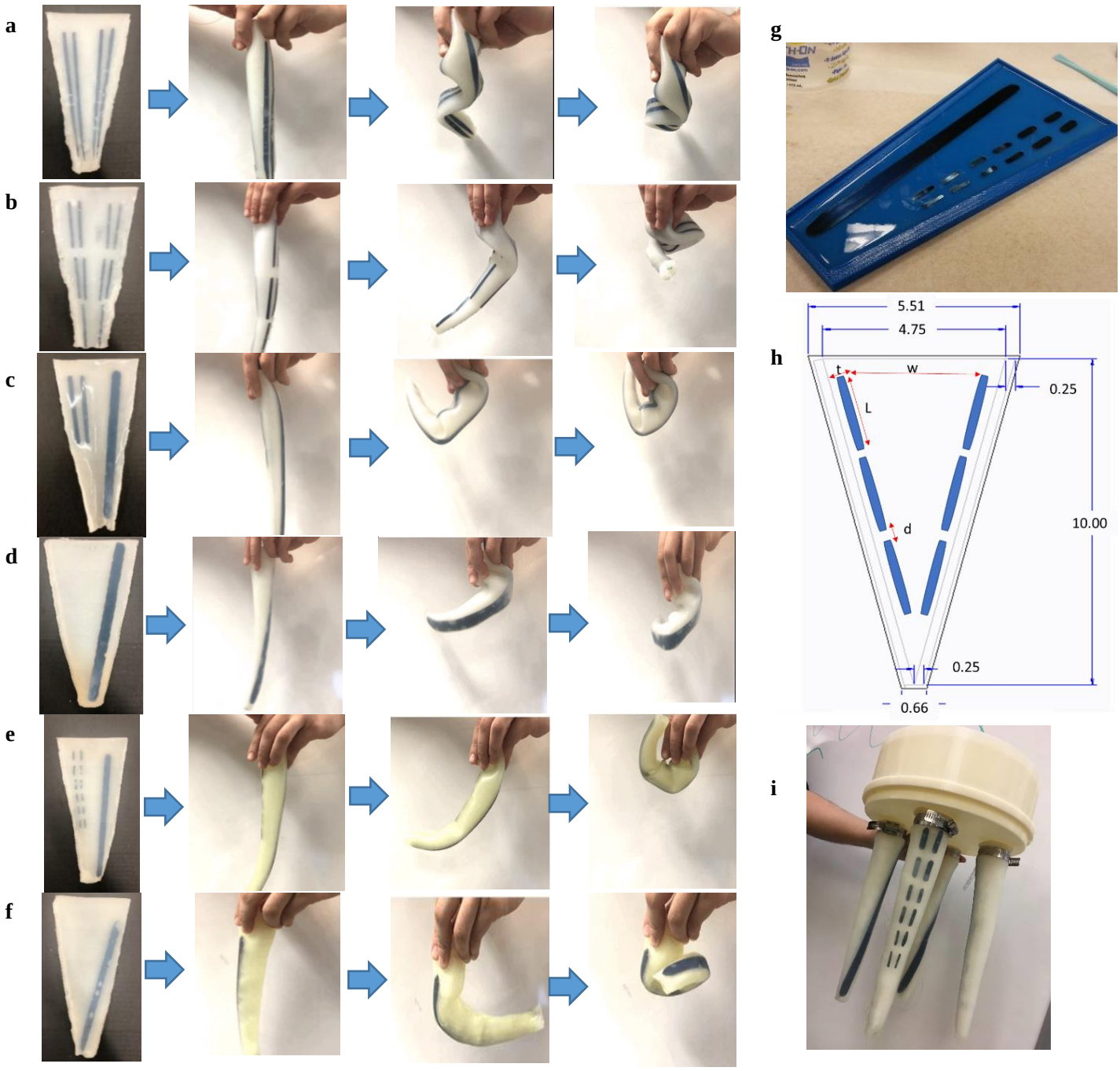

Fig. 2: **Different configuration of the octopus arm when spring steel, silicone and filler materials are changed: (a)** Double full length with no filler. **(b)** Sectioned double full length with no filler. **(c)** half length on one side and full length on other side with no filler added. **(d)** full length added on one side with no filler. **(e)** sectional half-length on one side and single full length on the other side with no filler added. **(f)** single full length added diagonally with filler. **Molding method and assembly**: **(g)** Sample of spring steel embedded in silicone. **(h)** A schematics of octopus arm mold in (inches). In the figure, *t* is the thickness of the spring steel, *L* is the length, *d* is the distance, *n* is the number of spring steels embedded. **(i)** Different arm configurations mounted on the structure.

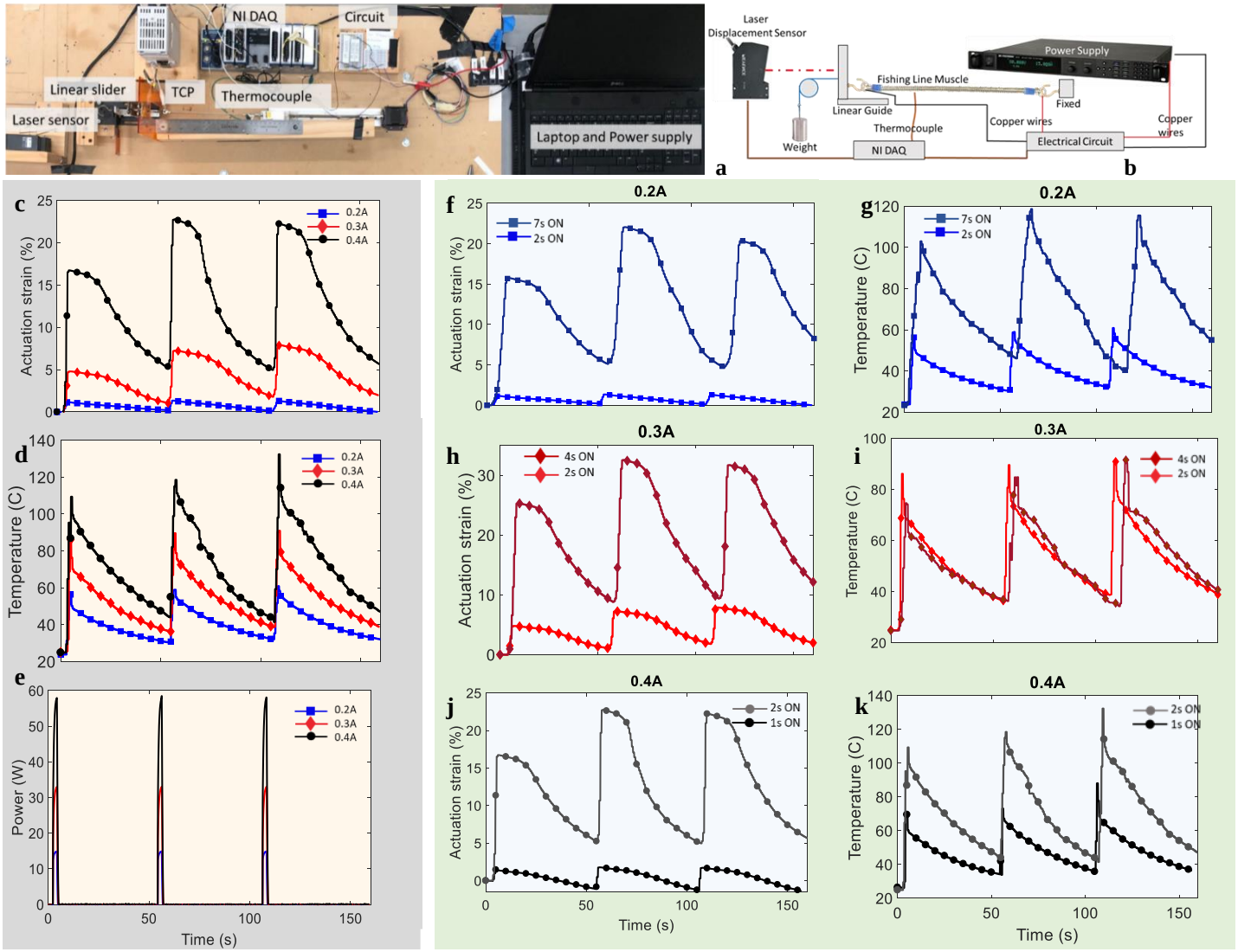

Fig. 3: Experimental characterization of self-coiled with nichrome TCP$_{FL}$ actuator. (a) Isotonic test experimental set up. (**b)** Experimental schematics. (**c-e)** 3 cycles experimental results at 2s ON and 50s OFF for 0.2A,0.3A, and 0.4A input current. (**c)** Actuation strain. (**d)** Temperature (**e)** Power. **(f-g)** Effect of heating time on actuation strain and temperature for 0.2A (**h-i**) for 0.3A, (**j-k**) for 0.4A. Markers are skipped at 50 points. All experiments presented here are taken at 10Hz data sampling time.

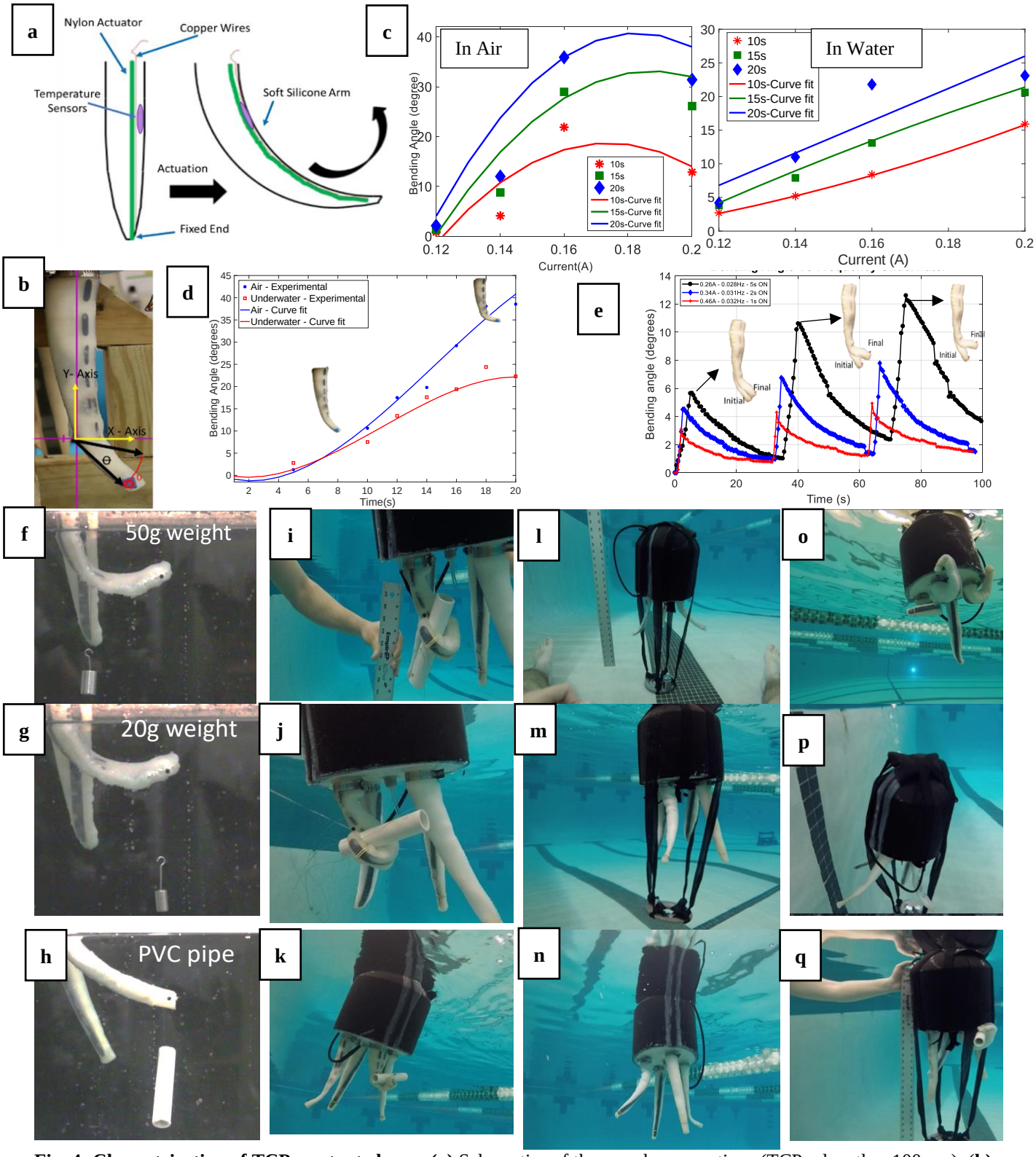

Fig. 4: Charactrization of TCP_{FL} actuated arm. (a) Schematics of the muscle connections (TCP_{FL} length = 100mm). (**b)** TCP octopus arm showing bending angle**.** (**c)** Bending angle vs input current at different time points. **(d)** Bending angle vs time at input current of 0.16A in air and in underwater condition. Tested in air and in underwater conditions**. (e)** Cyclic underwater actuation for low, medium, and high input current with variation of duty cycles**. Experimental TCP_{FL} silicone arm grasping objects in a 70-gallon fish tank** (**f-g)** 50g and 20g calibrated weight hanging on a wire. (**h)** Small PVC hooked on a wire. **Kraken deployed in a swimming pool (depth 6ft) actuated by stepper motors** (**i,j,k)** Grapsing of PVC pipe. **(l,m,n)** Arms in resting position while carrying 2.5kg payload. (**o)** Curling of octopus arms.(**p)** Bouyancy system releasing air, robot sinking. (**q)** Floating while grasping PVC with 2.5kg payload

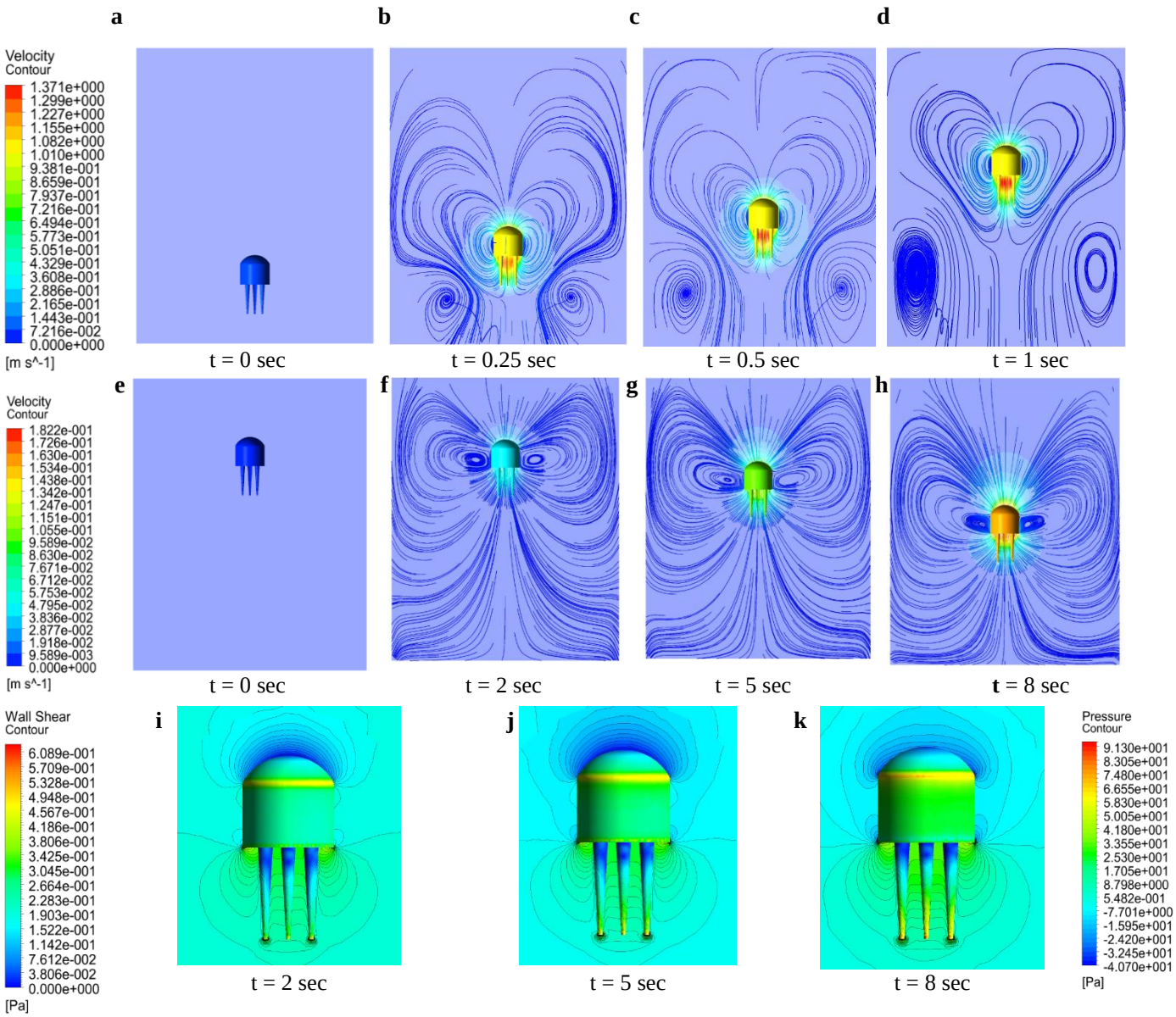

Fig. 5: Flow simulation for Kraken. (a-d) Flow field generated around the Kraken moving up with constant speed of 1m/s at various times**. (e-h)** Flow field generated around the Kraken accelerating downwards at 0.0198 m/s^2 at various times. **(i-k)** Pressure contours around and wall shear on surface of Kraken accelerating downwards at various times.

References

1. Haines, C.S., Lima, M.D., Li, N., Spinks, G.M., Foroughi, J., Madden, J.D., Kim, S.H., Fang, S., de Andrade, M.J., Göktepe, F.: Artificial muscles from fishing line and sewing thread. science **343**(6173), 868-872 (2014).
2. Haines, C.S., Li, N., Spinks, G.M., Aliev, A.E., Di, J., Baughman, R.H.: New twist on artificial muscles. Proceedings of the National Academy of Sciences **113**(42), 11709-11716 (2016).
3. Almubarak, Y., Tadesse, Y.: Twisted and coiled polymer (TCP) muscles embedded in silicone elastomer for use in soft robot. International Journal of Intelligent Robotics and Applications **1**(3), 352-368 (2017).
4. Saharan, L., Andrade, M.J.d., Saleem, W., Baughman, R.H., Tadesse, Y.: iGrab: Hand Orthosis Powered by Twisted and Coiled Polymer Muscles. Smart Materials and Structures (2017).
5. Wu, L., de Andrade, M.J., Saharan, L.K., Rome, R.S., Baughman, R.H., Tadesse, Y.: Compact and low-cost humanoid hand powered by nylon artificial muscles. Bioinspiration & biomimetics **12**(2), 026004 (2017).
6. Walker, I.D.: Continuous backbone "continuum" robot manipulators. Isrn robotics **2013** (2013).
7. Walker, I.D., Dawson, D.M., Flash, T., Grasso, F.W., Hanlon, R.T., Hochner, B., Kier, W.M., Pagano, C.C., Rahn, C.D., Zhang, Q.M.: Continuum robot arms inspired by cephalopods. In: Unmanned Ground Vehicle Technology VII 2005, pp. 303-315. International Society for Optics and Photonics
8. Menciassi, A., Gorini, S., Pernorio, G., Weiting, L., Valvo, F., Dario, P.: Design, fabrication and performances of a biomimetic robotic earthworm. In: Robotics and Biomimetics, 2004. ROBIO 2004. IEEE International Conference on 2004, pp. 274-278. IEEE
9. Wu, L., Chauhan, I., Tadesse, Y.: A Novel Soft Actuator for the Musculoskeletal System. Advanced Materials Technologies **3**(5), 1700359 (2018).
10. Walker, I.: Some issues in creating "invertebrate" robots. In: Proceedings of the International Symposium on Adaptive Motion of Animals and Machines 2000. Citeseer
11. Saharan, L., Tadesse, Y.: Robotic hand with locking mechanism using TCP muscles for applications in prosthetic hand and humanoids. In: Bioinspiration, Biomimetics, and Bioreplication 2016 2016, p. 97970V. International Society for Optics and Photonics
12. Wu, L., Jung de Andrade, M., Saharan, L., , Rome, R., Baughman, R., Tadesse, Y.: Compact and Low-cost Humanoid Hand Powered by Nylon Artificial Muscles. Bioinspiration & Biomimetics **12** (2) (2017). doi:10.1088/1748-3190/aa52f8
13. Tsukagoshi, H., Kitagawa, A., Segawa, M.: Active hose: An artificial elephant's nose with maneuverability for rescue operation. In: Robotics and Automation, 2001. Proceedings 2001 ICRA. IEEE International Conference on 2001, pp. 2454-2459. IEEE
14. Simeonov, A., Henderson, T., Lan, Z., Sundar, G., Factor, A., Zhang, J., Yip, M.: Bundled Super-Coiled Polymer Artificial Muscles: Design, Characterization, and Modeling. IEEE Robotics and Automation Letters **3**(3), 1671-1678 (2018).
15. Morimoto, Y., Onoe, H., Takeuchi, S.: Biohybrid robot powered by an antagonistic pair of skeletal muscle tissues. Science Robotics **3**(18), eaat4440 (2018).
16. Nawroth, J.C., Lee, H., Feinberg, A.W., Ripplinger, C.M., McCain, M.L., Grosberg, A., Dabiri, J.O., Parker, K.K.: A tissue-engineered jellyfish with biomimetic propulsion. Nature biotechnology **30**(8), 792 (2012).
17. Mintchev, S., Shintake, J., Floreano, D.: Bioinspired dual-stiffness origami. Science Robotics **3**(20), eaau0275 (2018).
18. Tomar, A., Tadesse, Y.: Multi-layer robot skin with embedded sensors and muscles. In: Electroactive Polymer Actuators and Devices (EAPAD) 2016 2016, p. 979809. International Society for Optics and Photonics
19. Stiehl, W.D., Lalla, L., Breazeal, C.: A" somatic alphabet" approach to" sensitive skin". In: Robotics and Automation, 2004. Proceedings. ICRA'04. 2004 IEEE International Conference on 2004, pp. 2865-2870. IEEE
20. Sanford, J., Ranatunga, I., Popa, D.: Physical human-robot interaction with a mobile manipulator through pressure sensitive robot skin. In: Proceedings of the 6th International Conference on Pervasive Technologies Related to Assistive Environments 2013, p. 60. ACM
21. Byun, J., Lee, Y., Yoon, J., Lee, B., Oh, E., Chung, S., Lee, T., Cho, K.-J., Kim, J., Hong, Y.: Electronic skins for soft, compact, reversible assembly of wirelessly activated fully soft robots. Science Robotics **3**(18), eaas9020 (2018).
22. Calisti, M., Arienti, A., Giannaccini, M.E., Follador, M., Giorelli, M., Cianchetti, M., Mazzolai, B., Laschi, C., Dario, P.: Study and fabrication of bioinspired octopus arm mockups tested on a multipurpose platform. In: Biomedical Robotics and Biomechatronics (BioRob), 2010 3rd IEEE RAS and EMBS International Conference on 2010, pp. 461-466. IEEE
23. Edwards, P., Pálsson, H.: Arrow-Odd: a medieval novel. New York University Press New York, (1970)
24. Katzschmann, R.K., DelPreto, J., MacCurdy, R., Rus, D.: Exploration of underwater life with an acoustically controlled soft robotic fish. (2018).
25. Coral, W., Rossi, C., Curet, O.M., Castro, D.: Design and assessment of a flexible fish robot actuated by shape memory alloys. Bioinspiration & biomimetics **13**(5), 056009 (2018).

26. Villanueva, A., Smith, C., Priya, S.: A biomimetic robotic jellyfish (Robojelly) actuated by shape memory alloy composite actuators. Bioinspiration & biomimetics **6**(3), 036004 (2011).
27. Tadesse, Y., Villanueva, A., Haines, C., Novitski, D., Baughman, R., Priya, S.: Hydrogen-fuel-powered bell segments of biomimetic jellyfish. Smart Materials and Structures **21**(4), 045013 (2012).
28. Frame, J., Lopez, N., Curet, O., Engeberg, E.D.: Thrust force characterization of free-swimming soft robotic jellyfish. Bioinspiration & biomimetics **13**(6), 064001 (2018).
29. Joshi, A., Kulkarni, A., Tadesse, Y.: FludoJelly: Experimental Study on Jellyfish-Like Soft Robot Enabled by Soft Pneumatic Composite (SPC). Robotics **8**(3), 56 (2019).
30. Joey, Z.G., Calderón, A.A., Chang, L., Pérez-Arancibia, N.O.: An earthworm-inspired friction-controlled soft robot capable of bidirectional locomotion. Bioinspiration & biomimetics **14**(3), 036004 (2019).
31. Liu, H., Curet, O.: Swimming performance of a bio-inspired robotic vessel with undulating fin propulsion. Bioinspiration & biomimetics **13**(5), 056006 (2018).
32. Mather, J.A.: How do octopuses use their arms? Journal of Comparative Psychology **112**(3), 306 (1998).
33. Kazakidi, A., Kuba, M., Botvinnik, A., Sfakiotakis, M., Gutnick, T., Hanassy, S., Levy, G., Ekaterinaris, J.A., Flash, T., Hochner, B.: Swimming patterns of the octopus vulgaris. In: 22nd Annual Meeting NCM Society 2012, pp. 23-29
34. Sfakiotakis, M., Kazakidi, A., Pateromichelakis, N., Tsakiris, D.P.: Octopus-inspired eight-arm robotic swimming by sculling movements. In: Robotics and Automation (ICRA), 2013 IEEE International Conference on 2013, pp. 5155-5161. IEEE
35. Sfakiotakis, M., Kazakidi, A., Tsakiris, D.: Octopus-inspired multi-arm robotic swimming. Bioinspiration & biomimetics **10**(3), 035005 (2015).
36. Arienti, A., Calisti, M., Giorgio-Serchi, F., Laschi, C.: PoseiDRONE: design of a soft-bodied ROV with crawling, swimming and manipulation ability. In: Oceans-San Diego, 2013 2013, pp. 1-7. IEEE
37. Serchi, F.G., Arienti, A., Laschi, C.: Biomimetic vortex propulsion: toward the new paradigm of soft unmanned underwater vehicles. IEEE/ASME Transactions On Mechatronics **18**(2), 484-493 (2013).
38. Festo: OctopusGripper and BionicCobot (undated). https://www.festo.com/group/en/cms/12745.htm
39. Fras, J., Noh, Y., Macias, M., Wurdemann, H., Althoefer, K.: Bio-inspired octopus robot based on novel soft fluidic actuator. In: 2018 IEEE International Conference on Robotics and Automation (ICRA) 2018, pp. 1583-1588. IEEE
40. Calisti, M., Giorelli, M., Levy, G., Mazzolai, B., Hochner, B., Laschi, C., Dario, P.: An octopus-bioinspired solution to movement and manipulation for soft robots. Bioinspiration & biomimetics **6**(3), 036002 (2011).
41. Sfakiotakis, M., Kazakidi, A., Tsakiris, D.P.: Turning maneuvers of an octopus-inspired multi-arm robotic swimmer. In: Control & Automation (MED), 2013 21st Mediterranean Conference on 2013, pp. 1343-1349. IEEE
42. Sfakiotakis, M., Kazakidi, A., Chatzidaki, A., Evdaimon, T., Tsakiris, D.P.: Multi-arm robotic swimming with octopus-inspired compliant web. In: Intelligent Robots and Systems (IROS 2014), 2014 IEEE/RSJ International Conference on 2014, pp. 302-308. IEEE
43. Laschi, C., Cianchetti, M., Mazzolai, B., Margheri, L., Follador, M., Dario, P.: Soft robot arm inspired by the octopus. Advanced Robotics **26**(7), 709-727 (2012).
44. Mazzolai, B., Margheri, L., Cianchetti, M., Dario, P., Laschi, C.: Soft-robotic arm inspired by the octopus: II. From artificial requirements to innovative technological solutions. Bioinspiration & biomimetics **7**(2), 025005 (2012).
45. Cianchetti, M., Calisti, M., Margheri, L., Kuba, M., Laschi, C.: Bioinspired locomotion and grasping in water: the soft eight-arm OCTOPUS robot. Bioinspiration & biomimetics **10**(3), 035003 (2015).
46. Thuruthel, T.G., Falotico, E., Renda, F., Flash, T., Laschi, C.: Emergence of behavior through morphology: a case study on an octopus inspired manipulator. Bioinspiration & Biomimetics **14**(3), 034001 (2019).
47. Salazar, R., Campos, A., Fuentes, V., Abdelkefi, A.: A review on the modeling, materials, and actuators of aquatic unmanned vehicles. Ocean Engineering **172**, 257-285 (2019).
48. Salazar, R., Fuentes, V., Abdelkefi, A.: Classification of biological and bioinspired aquatic systems: A review. Ocean Engineering **148**, 75-114 (2018).
49. Semochkin, A.N.: A device for producing artificial muscles from nylon fishing line with a heater wire. In: Assembly and Manufacturing (ISAM), 2016 IEEE International Symposium on 2016, pp. 26-30. IEEE
50. Yue, C., Guo, S., Li, M.: ANSYS FLUENT-based modeling and hydrodynamic analysis for a spherical underwater robot. In: Mechatronics and Automation (ICMA), 2013 IEEE International Conference on 2013, pp. 1577-1581. IEEE
51. Leong, Z.Q., Ranmuthugala, D., Penesis, I., Nguyen, H.D.: Computational fluid dynamics re-mesh method to generating hydrodynamic models for maneuvering simulation of two submerged bodies in relative motion. Journal of Computer Science and Cybernetics **27**(4), 353-362 (2011).
52. Leo, D.J.: Engineering Analysis of Smart Material Systems, vol. 1st Edition. John Wiley and sons Inc., Hoboken, New Jersey USA (2007)

53. LLC, m.: Nichrome 70-30 Medium Temperature Resistor Material. http://www.matweb.com/search/DataSheet.aspx?MatGUID=70c6833687d54cb4a000bd49ffd8e86c&ckck=1 . 2018
54. Yip, M.C., Niemeyer, G.: High-performance robotic muscles from conductive nylon sewing thread. In: 2015 IEEE International Conference on Robotics and Automation (ICRA) 2015, pp. 2313-2318. IEEE
55. Tadesse, Y., Thayer, N., Priya, S.: Tailoring the response time of shape memory alloy wires through active cooling and pre-stress. Journal of Intelligent Material Systems and Structures **21**(1), 19-40 (2010).
56. ANSYS.Inc.
57. Shepherd, R.F., Ilievski, F., Choi, W., Morin, S.A., Stokes, A.A., Mazzeo, A.D., Chen, X., Wang, M., Whitesides, G.M.: Multigait soft robot. Proceedings of the National Academy of Sciences **108**(51), 20400-20403 (2011).
58. Zhang, F., Thon, J., Thon, C., Tan, X.: Miniature underwater glider: Design, modeling, and experimental results. In: 2012 IEEE International Conference on Robotics and Automation 2012, pp. 4904-4910. IEEE
59. Zhou, H., Hu, T., Xie, H., Zhang, D., Shen, L.: Computational and experimental study on dynamic behavior of underwater robots propelled by bionic undulating fins. Science China Technological Sciences **53**(11), 2966-2971 (2010).

Acknowledgments

The authors would like to thank Davis Fletcher, Anthony Reyes, Hieu Doan, Norman Peters for their great contribution to the design and development of the robot in their senior design project. Armita Hamidi and Jeremy Warren for their comments and discussion. We would like to dedicate this study in the loving memory of Hieu Doan who lost his life recently (1997-2019).

Funding: The authors would like to acknowledge the support of the Office of Naval Research (ONR), Young Investigator Program, under Grant No. N00014-15-1-2503.

Authors contributions: Y.A., M.S., M.P., designed the robot. Y.A. contributed to experimental results and analysis of the TCP actuator and arm actuation. M.S., M.P conducted the swimming pool experimental test. S.S contributed to the modeling and computational fluid analysis. Y.T. conceived the idea of the robot, bioinspiration and led the project**.** All authors conceived the experimental work, wrote the paper, and provided feedback.

Competing interest: The authors declare they have no competing interests.

SUPPLEMENTARY MATERIALS

Fig. S1: Examples of presented octopus like robot found in the literature.
Fig. S2: Fabrication of fishing line muscle with thin heating wire
Fig. S3: Muscle characterization isotonic test set up
Fig. S4: Connectivity diagram of the robot's components.
Fig. S5: Steps of molding the silicone arm, assembling robot, and water sealing.
Fig. S6: Schematics of robot's controlling circuit.
Fig. S7: Computational domain of interest for the flow simulation, meshed model, and a snippet of the user-defined function (UDF) used for assigning the motion of the model.
Fig. S8: Experimental set up for TCP actuated arm (underwater and in air).
Fig. S9: Finite element analysis for 3D printed structure due to change of surrounding pressure.

Movie 1	Kraken, octopus like robot deployed for underwater testing in an Olympic size swimming pool. https://youtu.be/Hjv_z-EOwW8
Movie 2	Kraken, octopus robot fully functioning in a swimming pool. Grasping objects utilizing stepper motor hybrid actuation system. https://youtu.be/Tf8EwqJO1Vw
Movie 3	Kraken, octopus robot buoyancy system test for vertical swimming in a swimming pool (sinking and floating) https://youtu.be/UAuI5uTm59A
Movie 4	Kraken's designed six soft silicone arms showing the effect of stiffness on grasping modalities. https://youtu.be/g9l0Orj4ojo
Movie 5	Under water cyclic actuation at 0.032Hz frequency (input current of 0.26A with 5s heating) of the self-coiled twisted and coiled polymer fishing line actuator embedded silicone octopus arm. https://youtu.be/pEfsrprXY7Y
Movie 6	Underwater actuation of the self-coiled fishing line actuator arm at various input currents (0.12A-0.2A) https://youtu.be/1bI2ZaZf28w
Movie 7	Underwater grasping of objects such as a PVC pipe, 8.4oz filled can, and calibrated weight using the self-coiled fishing line actuator arm https://youtu.be/gyat05d1lPE

Movie 8 Kraken octopus robot deployed in the swimming pool displaying multiple functionalities such as grasping and releasing and curling of multiple arms, highlighting the safe human interaction aspect of this robot.
https://youtu.be/z2dfYvrlkaE

Movie 9 Fabrication process of self-coiled fishing line actuator.
https://youtu.be/LtMKnp6tuhM